Fermilab

Fermi National Accelerator Laboratory
P.O. Box 500 • Batavia, Illinois • 60510

TD-00-053

Magnetic Field Measurements of HGQ009 – Test Summary Report V1.00

P. Bauer, J. DiMarco, H. Glass, V. Kashikhin, G. Sabbi, P. Schlabach, G.Velev

September 14, 2000

Contents

List of Figures

List of Tables

1 Introduction

This report presents preliminary results of measurements of the magnetic field of HGQ009 made at the FNAL Vertical Magnet Test Facility in February-March of 2000. HGQ009 is the last 70 mm-aperture, short model LHC quadrupole built and tested at FNAL. We report only on magnetic measurements. Other aspects of the test program will be reported separately.

After a brief description of the measurement apparatus and program, we present relevant summaries of harmonics, comparisons to the previous magnets (mostly HGQ005) and other items of interest.

Magnetic measurements of HGQ009 were performed during two test cycles, most during the first. Between the first and second test cycles, the VMTF dewar was warmed to room temperature, but the magnet was not removed.

2 Measurement Apparatus, Analysis

Magnetic measurements of HGQ009 were made and analyzed using the system described in [1], [2]. A probe with nominal diameter 4.1 cm and length 0.8 m ("long" probe) has been used.

Note that measurement in the return end is limited by the length of the warm bore. There is no such mechanical restriction at the lead end. Therefore the smallest z position at which the "long" probe can be positioned is 0.255 m at the return end. In this position, the far end of the probe windings is approximately 0.2 m beyond the return end of the magnet, approximately 3 times the 70 mm magnet aperture. One would thus expect to capture nearly all of the magnet end field. At the lead end we expect that at a z position of about 1.9 m, the probe windings are entirely out of the body of the magnet.

In addition to the "long" probe measurements, a longitudinal integral scans were made using a probe with 25 mm nominal diameter and 4.3 cm length ("short" probe). The smallest z position at which the probe can be positioned is -0.078 m at the return end.

Field harmonics are computed at a reference radius of 17 mm. The measurement coordinate system is described in [4].

Further system, operations, and analysis information is available at

http://tsmtf.fnal.gov/~dimarco/sscl_systems.html.

3 Measurement Program

The list of measurements is given in Table 1. Measurements were concentrated on axial variation of field and current; time, and ramp rate dependence of harmonics. All 1.9K measurements were preceded by a 11kA heater induced quench.

In addition to the previous measured magnets a whole z-scan integral of HGQ009 was taken. This measurement was performed with the short and long probes at 1.9K and room temperature. Thus gave us possibility to determinate warm-to-cold change of the magnetic length.

This report highlights the main topics of the measurements. A more complete set of plots and tables are found at

4 Transfer Function and Field Angle

Figure 1a shows the transfer function obtained from measurements 2kA_zscan and 6kA_zscan. The average values at z=0.75 m (close to the geometrical center of the magnet) are 18.405 and 18.296 T/m/kA respectively.

The final yoke design for magnet HGQ009 adds the nominal magnetic component of the shims, introduced in magnets HGQ001-5, directly to the lamination. Therefore we can expect that the transfer function measured in HGQ009 agrees well with that of early magnets. For example the transfer function for magnet HGQ005 is 18.408 and 18.283 T/m/kA for 2kA_zscan and 6kA_zscan respectively.

Figure 1b shows the field angle as a function of z. The average magnet twist is about $\sim$ 1.1 mrad/m.

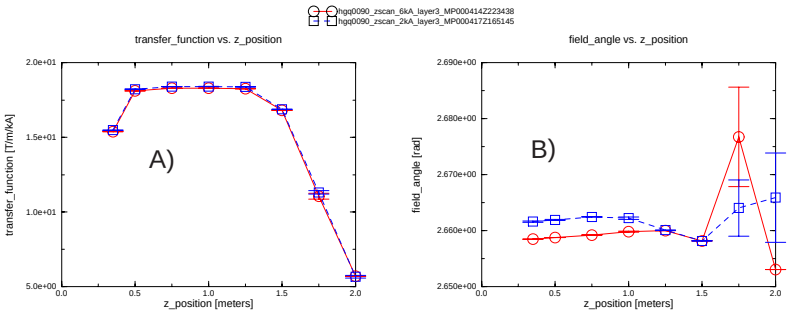

Figure 1: Transfer function and field angle.

5 Standard Harmonics

Tables 2-6 summarize the field harmonics in the magnet body. Data are from measurement r0400_13000Ah20 (test cycle one) taken at $z = 0.819$ m.

No.	File name	Explanation
1	collared_coil	Axial scan of collared coil (warm, FE1 probe)
2	yoked	Axial scan of cold mass (warm, FE1 probe)
3	long_probe_2kA_zscan	Axial scan at 2 kA, 1.9 K, TCI
4	long_probe_6kA_zscan	Axial scan at 6 kA, 1.9 K, TCI
5	long_probe_12500_zscan	Axial scan at 13 kA, 1.9 K, TCI
6	r0400_12500Ah10	Loop to 13 kA, 10 A/s, 1.9 K, TCI
7	r0400_12500Ah20	Loop to 13 kA, 20 A/s, 1.9 K, TCI
8	r0400_12500Ah40	Loop to 13 kA, 40 A/s, 1.9 K, TCI
9	r0400_12000Ah80	Loop to 13 kA, 80 A/s, 1.9 K, TCI
10	X1r12500Af10w00s30	Accelerator cycle with 10 min. 12.5 kA precycle current, 1.9 K, TCI
11	Stair0_12500As1000w02h20	Stair-step loop to 13 kA, 1.9 K, TCI)
12	X1r11000Af10w00s30	Accelerator cycle with 10 min. 11 kA precycle current, 1.9 K, TCI
13	X1r12500Af02w00s30	Accelerator cycle with 2 min. 12.5 kA precycle current, 1.9 K, TCI
14	r0400_12500Ah20_1_0564	Loop to 12.5 kA, 20 A/s, 1.9 K, Z=1.056m, TCI
15	r0400_12500Ah20_0_706	Loop to 12.5 kA, 20 A/s, 1.9 K, Z=0.706m, TCI
16	lead_end_zscan_6kA	Lead endscan at 6 kA, 1.9 K, TCI
17	lead_end_zscan_12500	Lead endscan at 12.5 kA, 1.9 K, TCI
18	short_probe_integral_zscan_6kA	Short probe integral axial scan, starting point -0.078 m at 6 kA, TCI
19	int_long_6kA	Long probe integral axial scan, starting point 0.253 m at 6 kA, TCI
20	int_long_12500	Long probe integral axial scan, starting point 0.253 m at 12.5 kA, TCI
21	l_probe_zscan_warm	Axial scan between TCI and TCII (+/-10A, warm)
22	long_probe_2kA_zscan	Axial scan at 2 kA, 1.9 K, TCII
23	long_probe_6kA_zscan	Axial scan at 6 kA, 1.9 K, TCII
24	long_probe_6kA_zscan	Axial scan at 12.5 kA, 1.9 K, TCII
25	r0400_12500Ah10	Loop to 12.5 kA, 10 A/s, 1.9 K, TCII
26	r0400_12500Ah20	Loop to 12.5 kA, 20 A/s, 1.9 K, TCII
27	r0400_12500Ah40	Loop to 12.5 kA, 40 A/s, 1.9 K, TCII
28	r0400_12000Ah80	Loop to 12.5 kA, 80 A/s, 1.9 K, TCII
29	X1r12500Af10w00s30	Accel. cycle, 10 min. 13 kA flattop, 1.9 K, TCII
30	short_probe_zscan_6kA	Short probe integral axial scan at 6 kA, TCII
31	short_probe_zscan_12_5kA	Short probe integral axial scan at 12.5 kA, TCII
32	long_probe_int_6ka	Long probe integral axial scan at 6 kA, TCII
33	long_probe_int_12.5ka	Long probe integral axial scan at 12.5 kA, TCII
34	sp_zscan	Short probe integral axial scan at 36 A, after TCII

Table 1: The following magnetic measurements have been performed on HGQ009. Except where noted, all measurements with fixed probe position were made at Z=0.819 m (near magnet center).

Field Harmonics at 0.8 kA, test cycle one		
n	ramp up	ramp down
b_3	0.6693± 0.0431	0.6785± 0.0146
b_4	-0.0788± 0.0369	-0.0602± 0.0093
b_5	0.0991± 0.0269	0.1551± 0.0176
b_6	-2.0874± 0.6610	0.8336± 0.2986
b_7	0.0492± 0.0315	0.0695± 0.0037
b_8	-0.0060± 0.0154	-0.0128± 0.0023
b_9	0.0004± 0.0093	0.0063± 0.0016
b_{10}	0.0234± 0.0122	-0.0234± 0.0042
a_3	0.3567± 0.0267	0.3548± 0.0132
a_4	0.2392± 0.0401	0.1537± 0.0254
a_5	-0.1353± 0.0420	-0.1710± 0.0109
a_6	0.0984± 0.0307	0.0876± 0.0124
a_7	0.0148± 0.0279	0.0329± 0.0060
a_8	0.0179± 0.0074	0.0080± 0.0022
a_9	-0.0049± 0.0016	-0.0038± 0.0019
a_{10}	0.0003± 0.0024	0.0016± 0.0011

Table 2: Field harmonics at 0.8 kA measured during the first test cycle. Separate values are given for the field during up and down ramp. (Data are fitted with line over the range ±0.3 kA around the nominal value. The change in field with current over that range is small.) The quoted error is result from the linear fit at the nominal current.

The harmonic b_6 vs current for different ramp rates is shown on figure 2. One can see that the hysteresis width is increasing with the ramp rate but not by much as in the magnets HGQ006-8.

Harmonics through $n = 13$ are produced "automatically" by measuring system software. We have traditionally reported only through $n = 10$.

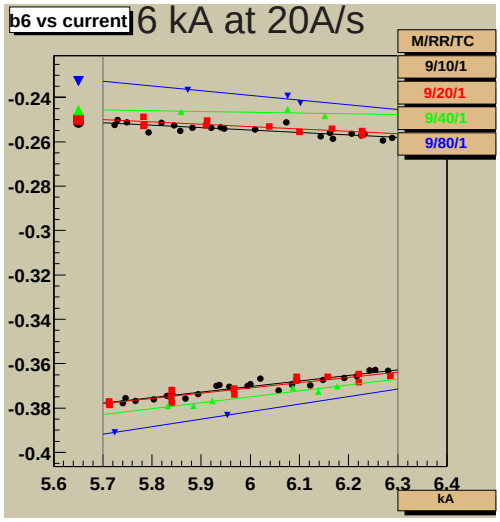

Figure 2: b_6 vs current at 6 kA for different ramp rates, 10, 20, 40 and 80 A/s. The lines represent a linear fit in the interval (5.7,6.3) kA.

Field Harmonics at 2 kA, test cycle one		
n	ramp up	ramp down
b_3	0.6913± 0.0064	0.6905± 0.0144
b_4	-0.0611± 0.0077	-0.0468± 0.0045
b_5	0.0870± 0.0040	0.1005± 0.0059
b_6	-0.7428± 0.0585	-0.0496± 0.0525
b_7	0.0544± 0.0016	0.0594± 0.0019
b_8	-0.0099± 0.0017	-0.0110± 0.0008
b_9	0.0019± 0.0007	0.0027± 0.0012
b_{10}	-0.0011± 0.0012	-0.0124± 0.0009
a_3	0.3523± 0.0073	0.3592± 0.0125
a_4	0.2921± 0.0133	0.2391± 0.0084
a_5	-0.1392± 0.0063	-0.1458± 0.0038
a_6	0.0550± 0.0023	0.0566± 0.0039
a_7	0.0142± 0.0023	0.0194± 0.0027
a_8	0.0139± 0.0010	0.0107± 0.0012
a_9	-0.0045± 0.0012	-0.0039± 0.0010
a_{10}	0.0005± 0.0008	0.0012± 0.0010

Table 3: Field harmonics at 2 kA measured during the first test cycle.

Field Harmonics at 6 kA, test cycle one		
n	ramp up	ramp down
b_3	0.6946± 0.0037	0.6928± 0.0033
b_4	-0.0411± 0.0026	-0.0375± 0.0019
b_5	0.0819± 0.0022	0.0844± 0.0017
b_6	-0.3709± 0.0050	-0.2532± 0.0024
b_7	0.0543± 0.0012	0.0554± 0.0009
b_8	-0.0103± 0.0009	-0.0111± 0.0010
b_9	0.0018± 0.0007	0.0020± 0.0008
b_{10}	-0.0074± 0.0005	-0.0091± 0.0003
a_3	0.3470± 0.0050	0.3437± 0.0033
a_4	0.2997± 0.0033	0.2753± 0.0023
a_5	-0.1383± 0.0033	-0.1372± 0.0014
a_6	0.0438± 0.0013	0.0447± 0.0014
a_7	0.0147± 0.0010	0.0171± 0.0016
a_8	0.0119± 0.0009	0.0112± 0.0010
a_9	-0.0043± 0.0009	-0.0034± 0.0006
a_{10}	0.0010± 0.0005	0.0013± 0.0004

Table 4: Field harmonics at 6 kA measured during the first test cycle.

Field Harmonics at 12 kA, test cycle one		
n	ramp up	ramp down
b_3	0.7108± 0.0038	0.7097± 0.0032
b_4	-0.0375± 0.0023	-0.0355± 0.0014
b_5	0.0773± 0.0011	0.0783± 0.0012
b_6	-0.3354± 0.0011	-0.3057± 0.0011
b_7	0.0541± 0.0008	0.0546± 0.0007
b_8	-0.0110± 0.0007	-0.0115± 0.0008
b_9	0.0012± 0.0004	0.0014± 0.0004
b_{10}	-0.0046± 0.0004	-0.0050± 0.0003
a_3	0.3516± 0.0042	0.3539± 0.0043
a_4	0.3001± 0.0015	0.2932± 0.0014
a_5	-0.1347± 0.0007	-0.1351± 0.0010
a_6	0.0380± 0.0011	0.0389± 0.0013
a_7	0.0165± 0.0012	0.0167± 0.0009
a_8	0.0116± 0.0007	0.0110± 0.0005
a_9	-0.0042± 0.0005	-0.0041± 0.0006
a_{10}	0.0012± 0.0003	0.0013± 0.0003

Table 5: Field harmonics at 12 kA measured during the first test cycle.

No. n	800 kA mean ± error	2000 kA mean ± error	6000 kA mean ± error	11000 kA mean ± error	12000 kA mean ± error
b_3	0.674± 0.1201	0.691± 0.0720	0.694± 0.0417	0.701± 0.0365	0.710± 0.0418
b_4	-0.070± 0.1075	-0.054± 0.0552	-0.039± 0.0335	-0.036± 0.0288	-0.037± 0.0306
b_5	0.127± 0.1055	0.094± 0.0496	0.083± 0.0313	0.078± 0.0244	0.078± 0.0236
b_6	-0.627± 0.4898	-0.396± 0.1666	-0.312± 0.0431	-0.320± 0.0253	-0.321± 0.0232
b_7	0.059± 0.0937	0.057± 0.0297	0.055± 0.0230	0.054± 0.0247	0.054± 0.0193
b_8	-0.009± 0.0665	-0.010± 0.0252	-0.011± 0.0219	-0.011± 0.0184	-0.011± 0.0194
b_9	0.003± 0.0521	0.002± 0.0217	0.002± 0.0190	0.001± 0.0149	0.001± 0.0140
b_{10}	0.000± 0.0641	-0.007± 0.0224	-0.008± 0.0141	-0.005± 0.0149	-0.005± 0.0129
a_3	0.356± 0.0999	0.356± 0.0704	0.345± 0.0455	0.346± 0.0463	0.353± 0.0460
a_4	0.196± 0.1280	0.266± 0.0736	0.288± 0.0377	0.293± 0.0335	0.297± 0.0271
a_5	-0.153± 0.1150	-0.142± 0.0501	-0.138± 0.0341	-0.135± 0.0260	-0.135± 0.0208
a_6	0.093± 0.1039	0.056± 0.0391	0.044± 0.0262	0.040± 0.0248	0.038± 0.0246
a_7	0.024± 0.0922	0.017± 0.0354	0.016± 0.0255	0.016± 0.0226	0.017± 0.0228
a_8	0.013± 0.0490	0.012± 0.0237	0.012± 0.0221	0.012± 0.0191	0.011± 0.0175
a_9	-0.004± 0.0296	-0.004± 0.0233	-0.004± 0.0196	-0.004± 0.0187	-0.004± 0.0162
a_{10}	0.001± 0.0298	0.001± 0.0207	0.001± 0.0147	0.001± 0.0120	0.001± 0.0127

Table 6: Field harmonics as measured during the first test cycle. Up and down ramp data are averaged.

6 Axial Scans

Figure 3 shows the variation in the low order normal harmonics along the magnet axis. The smallest z position at which the long probe was positioned was 0.35 m due to the depth of the warm bore. At the lead end, at a z position of 1.9 m, the probe windings are entirely out of the body of the magnet.

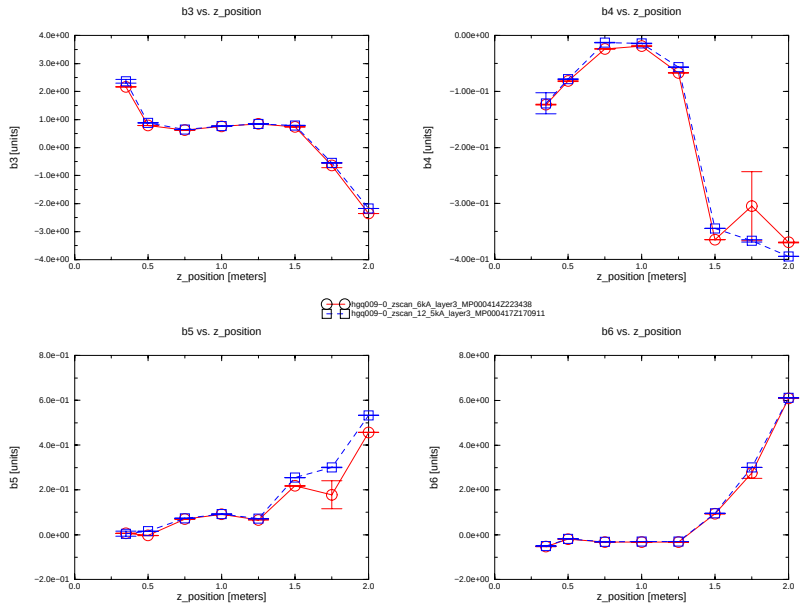

Figure 3: Multipoles b3 to b6 as a function of axial position z, measured at 6kA and 12.5kA.

There is little difference in the multipole content between 6kA and 12.5kA. Within the body, b_3-b_6 remain almost constant. For b_4, however, the transition from body to end occurs over a large region, starting about 0.75 m from the end.

7 Scan of Magnet Return End

Figure 4 shows the transfer function, field angle, and x- and y-centers at 6 kA and 12.5 kA in the lead end of the magnet. Data from the first test cycles are shown; there is a nice agreement between data, consistent with our expectation.

As a figure of merit we characterize the end field by the harmonics at z=2.0 m normalized to the body field (z=1.0 m).[1]

[1] At the 2 m position, the probe should see only end field where we define the end region as beginning at the transition from normal to full round collars.

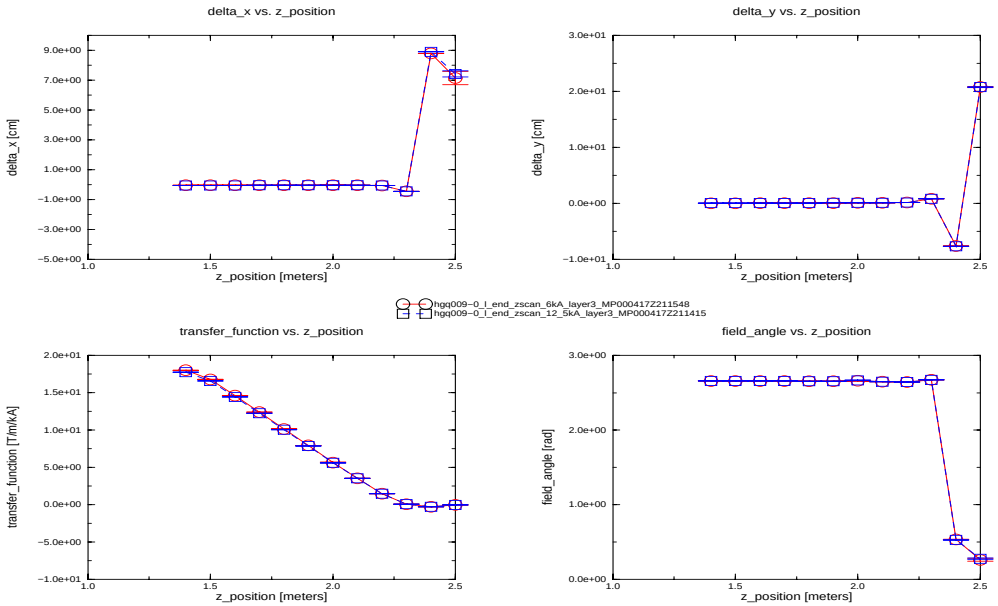

Figure 4: Transfer function, field angle and magnetic center as function of z in the lead end.

End field harmonics are given in Table 7 for HGQ005 (endscan_13000A_tc2) and HGQ009 (l_end_zscan_12_5kA). There is some variation from magnet to magnet in the sextupole, with the standard deviations of b_3 and a_3 being equal to 1.03 and 0.37 units, respectively. One also sees that b_6 in HGQ009 is somewhat larger than for HGQ005, but this could be expected, as a consequence of small design modifications [8].

Magnet	Ratio of TF	**Field Harmonics**								
		n=	3	4	5	6	7	8	9	10
HGQ009	0.31	b_n	-2.22	-0.33	0.45	5.89	0.03	-0.02	-0.06	-0.09
		a_n	0.01	2.37	-0.19	-0.73	-0.07	-0.05	-0.05	-0.01
HGQ005	0.04	b_n	0.38	0.16	-0.22	0.37	-0.01	0.00	0.00	-0.01
		a_n	0.51	0.13	-0.12	0.13	0.03	0.01	-0.02	0.00

Table 7: End field harmonics in HGQ009 and HGQ005 normalized to the body field strength. The ratio of field strength in the end to that in the body is also given.

8 Variation of Hysteresis with Cycle Number

It was observed for HGQ002,HGQ003 and somewhat for HGQ005 (but not for HGQ001) that b_6 hysteresis during the first up ramp differs from that of other cycles. For HGQ009, only a slight difference was observed. The difference between first and subsequent cycles for HGQ005 at 1000A was about 0.05 units. This difference is approximately the same for HGQ009. Measured dodecapole for first cycle loops from 800 to 12500 A at 20 A/s ramp rate is plotted in Fig. 5. The first cycle up ramp follows nearly an identical path to the second cycle.

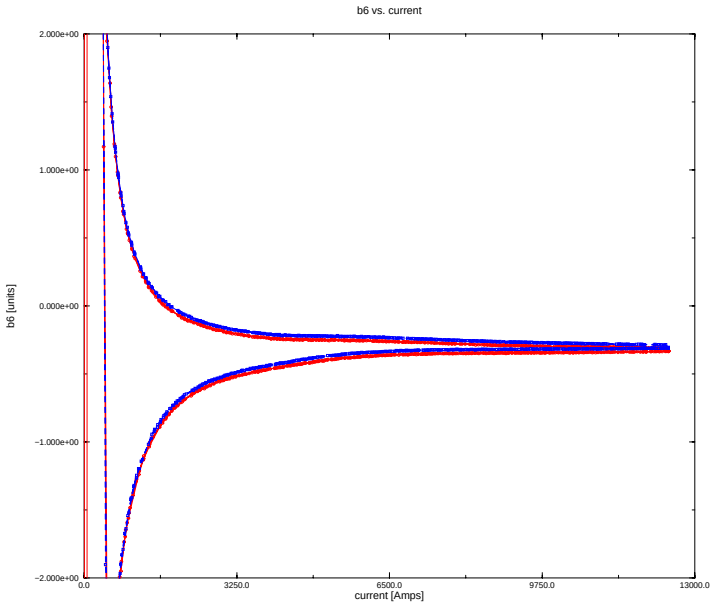

Figure 5: Measured b_6 during hysteresis loops. Data is taken from measurements r0800_12500Ah20, test cycles one and two.

9 Accelerator cycle ramps

Table 8 gives the change in harmonics during a 30 min. injection plateau at 800A for magnets HGQ009 (file hgq009-0_X1r12500Af10w00s30) and HGQ005 (file hgq005_X1r13000Af10w00s30). The change in b_6 of 0.13 units for HGQ009 is comparable with the 0.09 units seen in HGQ005. The change in HGQ009 a_4 is smaller than observed for HGQ005. All other HGQ009 changes during injection are small ($\leq$ 0.03 units).

	HGQ005		HGQ009	
n	Δb_n	Δa_n	Δb_n	Δa_n
3	-0.05 ± 0.03	-0.04 ± 0.02	-0.01± 0.03	0.07± 0.02
4	0.00 ± 0.01	-0.11 ± 0.01	-0.01± 0.01	-0.01± 0.01
5	0.01 ± 0.00	0.03 ± 0.01	0.00± 0.01	0.01± 0.01
6	0.09 ± 0.01	-0.01 ± 0.00	0.13± 0.02	-0.01± 0.01
7	0.00 ± 0.00	-0.01 ± 0.00	0.00± 0.00	0.00± 0.00
8	0.00 ± 0.00	0.00 ± 0.00	0.00± 0.00	0.00± 0.00
9	-0.00 ± 0.00	-0.00 ± 0.00	0.00± 0.00	0.00± 0.00
10	-0.01 ± 0.00	0.00 ± 0.00	-0.01± 0.01	0.00± 0.00

Table 8: Change in field during a 30 min. injection plateau. ($I = 800A$)

10 Comparison of Measurements Made During the Both Test Cycles

Measurements of HGQ009 were made in each of the two test cycles. Between test cycles one and two the magnet was warmed up to room temperature and cooled back down without removal.

The following changes in field were observed from the first test cycle to the second.

1. Transfer function measured in TC2 is reduced by 0.025% relative to TC1 (Fig. 6).
2. $\Delta b_6 = 9\%$ where $(\Delta b_n = (b_n^{TC2} - b_n^{TC1})/b_n^{TC2})$.
3. $\Delta b_{10} = -6\%$.
4. Some changes are observed in unallowed harmonics (e.g. $\Delta b_3 = -4\%$).

11 Result from Z-scan Integral Measurements Made During the First and Second Test Cycles

For the first time the whole body z-integral of the magnetic field was taken. The detailed measurement with the long and short probes was performed at 6 kA. The similar measurement was done in the TC2 but with reduced number of points for the short probe at 6 and 12.5 kA. At the end of the magnetic program, a warm measurement (I=±35.5 A) was taken.

Table 10 represents the comparison between long and short probes. The long probe data are from the point z=0.75 m. The short probe data are integrated over the z-interval (0.395,1.126) m. One can see that the harmonics measured with two different probes are in good agreement. The small differences are due to effects of cross-calibration between the probes and integration procedure.

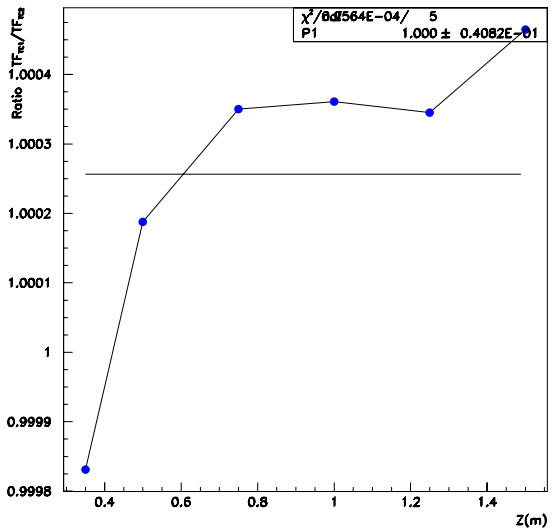

Figure 6: Comparison TF_{TC1}/TF_{TC2} at 6 kA.

n	**Cold Measurement** Integrated Short Probe	Long Probe
b_3	0.630	0.635
b_4	-0.035	-0.023
b_5	0.033	0.072
b_6	-0.318	-0.332
b_7	0.073	0.051
b_8	-0.023	-0.009
b_9	-0.015	0.000
b_{10}	-0.039	-0.007
a_3	0.382	0.360
a_4	0.251	0.276
a_5	-0.102	-0.150
a_6	0.061	0.037
a_7	0.026	0.022
a_8	0.028	0.012
a_9	-0.047	-0.004
a_{10}	0.024	0.001

Table 9: Field harmonics compared between short and long probes (flux analysis).

12 Determination of the Magnetic Filed Length. Comparison between Warm and Cold

The short probe measurement gives possibility to determinate the length of the magnetic filed. We found that the length of the HGQ009 magnetic filed is 1.7756 ± 0.0008 m. The next exercise is to compare the lead and return ends shapes to the ROXIE prediction. In average we have to translate with 0.137 m the simulated TF in the positive z direction to match the lead and return ends shapes with the measured ones (Fig. 7). In addition there is a difference of 2.7 cm between the return and lead ends shifts. This could indicate some problem in the computer model.

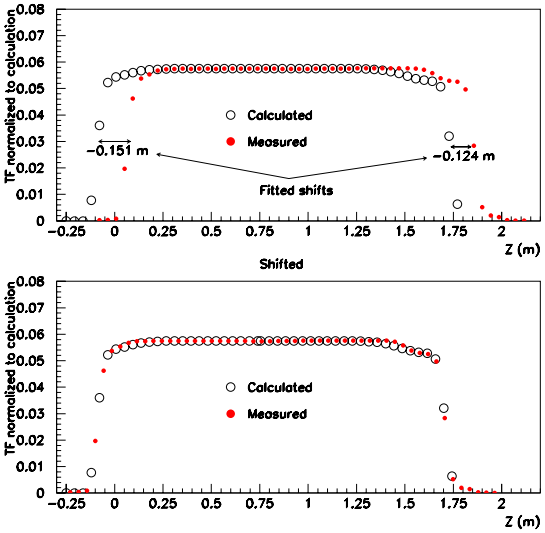

Figure 7: Comparison of TFs, read points are short probe data, circles are from ROXIE calculation.

Fig. 8 shows the comparison between cold and warm measurements of the transfer function. The difference between warm and cold magnetic field length is 5 mm, which one can expect from thermal shrinking of the coil [9].

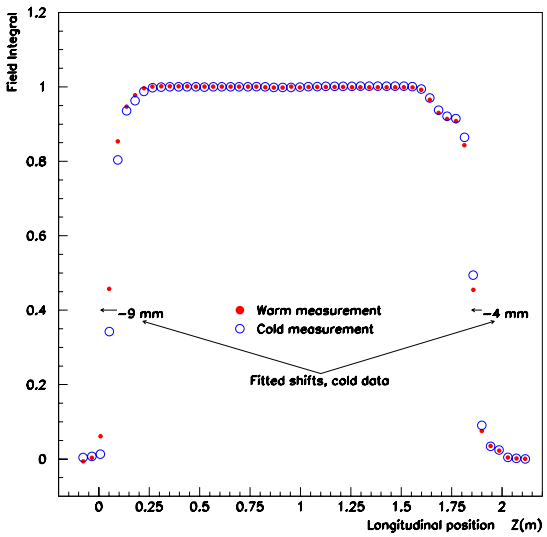

Figure 8: Comparison of TFs, cold and worm measurements.

13 Summary

We make the following observations about the magnet.

1. Normal and skew harmonics for $n \geq 7$ are less than 0.01-0.02 units in the body of the magnet. Table 10 summarizes field quality in the magnets HGQ005 and HGQ009 [7].

n	HGQ09	HGQ05
b_3	0.69	0.72
b_4	-0.04	0.00
b_5	0.08	-0.04
b_6	-0.31	-0.30
b_7	0.05	0.01
b_8	-0.01	0.00
b_9	0.00	0.00
b_{10}	-0.01	0.01
a_3	0.34	0.12
a_4	0.28	0.19
a_5	-0.13	0.05
a_6	0.04	-0.03
a_7	0.02	0.01
a_8	0.01	0.00
a_9	0.00	0.00
a_{10}	0.00	0.00

Table 10: Field harmonics measured at magnet center at 6 kA.

2. Harmonics show little change as a function of current. The biggest variations are 9% in b_6 and 4% in b_3.

3. There is no significant difference in the hysteresis loops between the first and second test cycles.

4. Using the "short" probe a precise measurement of the magnetic length was performed.

5. Comparing warm/cold "short" probe measurements, a difference of 5 mm was obtained. It is consistent with the thermal shrinking of the coil.

References

[1] J. DiMarco, *et. al.*, "HGQS01 Test Summary Report", TD-98-025, (1998)

[2] J. DiMarco, P. Schlabach, "Magnetic Field Measurements of HGQ002 – Test Summary Report", TD-98-045, (1998)

[3] J. DiMarco, P. Schlabach, "Magnetic Field Measurements of HGQ005 – Test Summary Report", TD-98-028, (1999)

[4] J. DiMarco, M. Lamm, G. Sabbi, P. Schlabach, "Conventions for HGQ Field Quality Representation", TD-98-036 , (1998)

[5] J. DiMarco, P. Schlabach, "Magnetic Field Measurements of HGQ003 – Test Summary Report", TD-98-058, (1998)

[6] P. Schlabach, "Analysis of Sextupole Field Distortions and Snapshot Events During Testing of HGQ001 and HGQ002", TD-98-056, (1998)

[7] N. Andreev, *et. al.*, "Field Quality of Quadrupole R & D Models for the LHC IR", PAC99, (1999)

[8] N. Andreev, *et. al.*, "Field Quality in Fermilab-build Models of High Gradient Quadrupole Magnets for the LHC Interaction Region", MT-16, (1999)

[9] Roger Rabehl, Private comunication.